Supplementary information for:

Atlantic atmospheric rivers and the pulse of deep Mediterranean respiration

1 A geochemical proxy for river clay discharge and rainfall on the Iberian Peninsula

IODP Site U1385 is located on a promontory offshore the continental slope of the Iberian Margin off Portugal. Sedimentary particulate matter reaches the site by two main routes[59]: (1) by vertical pelagic rain of suspended particles composed of biogenic carbonate microplankton and siliciclastic particles transported by river plumes or direct offshore windblown dust deposition; and (2) by intermediate and bottom nepheloid layers triggered by sediment resuspension in the outer shelf or along the slope. Terrestrial sedimentation on the distal setting of the IM depends on the frequency and sediment load of these bottom and intermediate nepheloid layers and on the extension of the surface nepheloid layer that depends on river sediment discharge and the offshore extension of the river plumes during flooding episodes[59].

Over the last 350 kyr, sedimentation along the IM was mainly driven by the balance between the relative accumulations of carbonate, which is mainly produced by pelagic calcareous plankton, and siliciclastic particulate matter delivered by rivers or windblown dust[13,15,40,60,61,62]. This balance, which has been measured through the Ti/Ca ratio and Natural Gamma Radiation (NGR), is very similar in Site U1385 located in the continental rise, below the influence of the MOW and Site U1389 drilled in the continental slope and greatly affected by the MOW[60] (Fig S1).

Terrestrial input to the IM was controlled by sea level and precession-driven changes in riverine discharge to the ocean[13,15,40,60,61,62] (Supplementary Fig. 1). Overall, terrestrial sedimentation tends to increase as sea level falls and the shoreline moves seaward, depositing sediments closer to the shelf break, and tends to decrease as sea level rises and

fluvial inputs remain in estuaries away from the outer shelf[15,60,61,62]. The fact that the higher sedimentation rates occur during periods of higher relative siliciclastic proportions indicates that it is probably changes in the rate of terrestrial inputs that exert the greatest control on the Ti/Ca and NGR, whereas carbonate flux tends to be more constant[61]. This accounts for the low Ti/Ca and NGR during highstands of the main interglacial periods (Supplementary Fig. 1). Another pattern common to most sites on the IM is that the Ti/Ca ratio and NGR tend to covary with insolation, regardless of whether these sites are affected by the MOW or not[13,15,40,60,61]. This is the case for example for sites U1385 and U1389 (Supplementary Fig. 1). Nevertheless, some differences in the Ti/Ca and NGR can be recognized between these two sites because the Ti/Ca and NGR were also driven by changes in marine carbonate productivity that varies with SST, increasing during the warm interstadial periods[15]. It is in the interstadial episodes during BSI maxima that a substantial difference is observed between the record of site U1385 and U1389 (Supplementary Fig. 1), while in the proximal site the Ti/Ca ratio remains high or decreases gradually, a sharp decrease is seen at U1385. The Ti/Ca ratio is driven by the relative changes in the local rates of terrestrial versus carbonate inputs. In the distal setting of site U1385 the relative change in the rate of siliciclastic supply is smaller compared to the change in carbonate productivity, while at U1389 the opposite is true (Supplementary Fig. 1).

To better understand the origin of the terrestrial fraction at Site U1385 we used the (Zr+Ti)/K ratio (Supplementary Fig. 1), focusing on the relative proportion of terrestrial minerals, while removing Ca to eliminate the effect of carbonate productivity. K and Al are concentrated in fine-grained, clay minerals carried by rivers and transported offshore in suspension by buoyant river plumes[12,64,65]. In contrast, Ti and Zr are concentrated in heavy, coarser minerals, such as zircon, titanite, rutile, etc, that have been related to windblown dust deposition transported from Saharan winds[66]. Heavy minerals can also be transported

by rivers, but they preferentially settle out on the inner shelf or are concentrated in turbidites because of hydrodynanic sorting related to their higher density[67]. For the same reason, Zr and Ti are concentrated by preferential sorting of heavy minerals caused by bottom currents. The ratio between clay-rich (Al and K-enriched particles) and heavy minerals (enriched in Ti and Zr) has been used as a proxy for riverine versus eolian input[12,64,65]. For example, low Ti/Al has been linked to humid periods during sapropel deposition[12,64,65]. In this study, we used the (Zr+Ti)/K record (Supplementary Fig. 1) instead of Ti/Al because measurements of Al by X-ray fluorescence is problematic because of its low mass and weak fluorescence. In general, the (Zr+Ti)/K parallels the BSI, with high mean values during low BSI and significant decreases during high BSI (Fig. 2a,b, Supplementary Fig. 1). We interpret the sediments poor in Zr and Ti and rich in K-bearing minerals as being due to fine-grained clay transported offshore by buoyant river plumes. These extensive river plumes reaching the location of Site U1385 were the result of river flooding and heavy precipitation on land. The dominance of clay minerals with low proportion of silty deposits rich in heavy minerals reflects particles settling vertically through the water column in distal settings. At site U1385, the lowest (Zr+Ti)/K ratio occurred during the periods of lower Ti/Ca ratio and higher carbonate content, synchronous with maximum BSI and minimum sedimentation rates (Supplementary Fig. 1). In contrast, the high (Zr+Ti)/K is indicative of vertical settling of windblown dust deposited offshore and/or derived from resuspension of sediments transported from the outer shelf or the slope (Supplementary Fig. 1). In both cases, the particles will be coarser and rich in heavy minerals and consequently enriched in Zr and Ti. Consequently, we relate the events of high (Zr+Ti)/K with enhanced dust input to the IM and/or increase transport by nepheloid layers originated by resuspension along the outer shelf or the slope. The similarity between the Zr/Rb record at Site U1385, drilled on the continental rise, and Site U1391 recovered on the continental slope of the IM has been

attributed to changes in MOW strength[68]. Given that the Zr/Rb ratio also reflects the relative proportion of silts and clay in sediments, as does the (Zr+Ti)/K ratio, this study assumes that the observed changes are the result of variations in terrigenous input from the continent, although hydrodynamic sorting by resuspension from bottom currents may also have exerted a small influence.

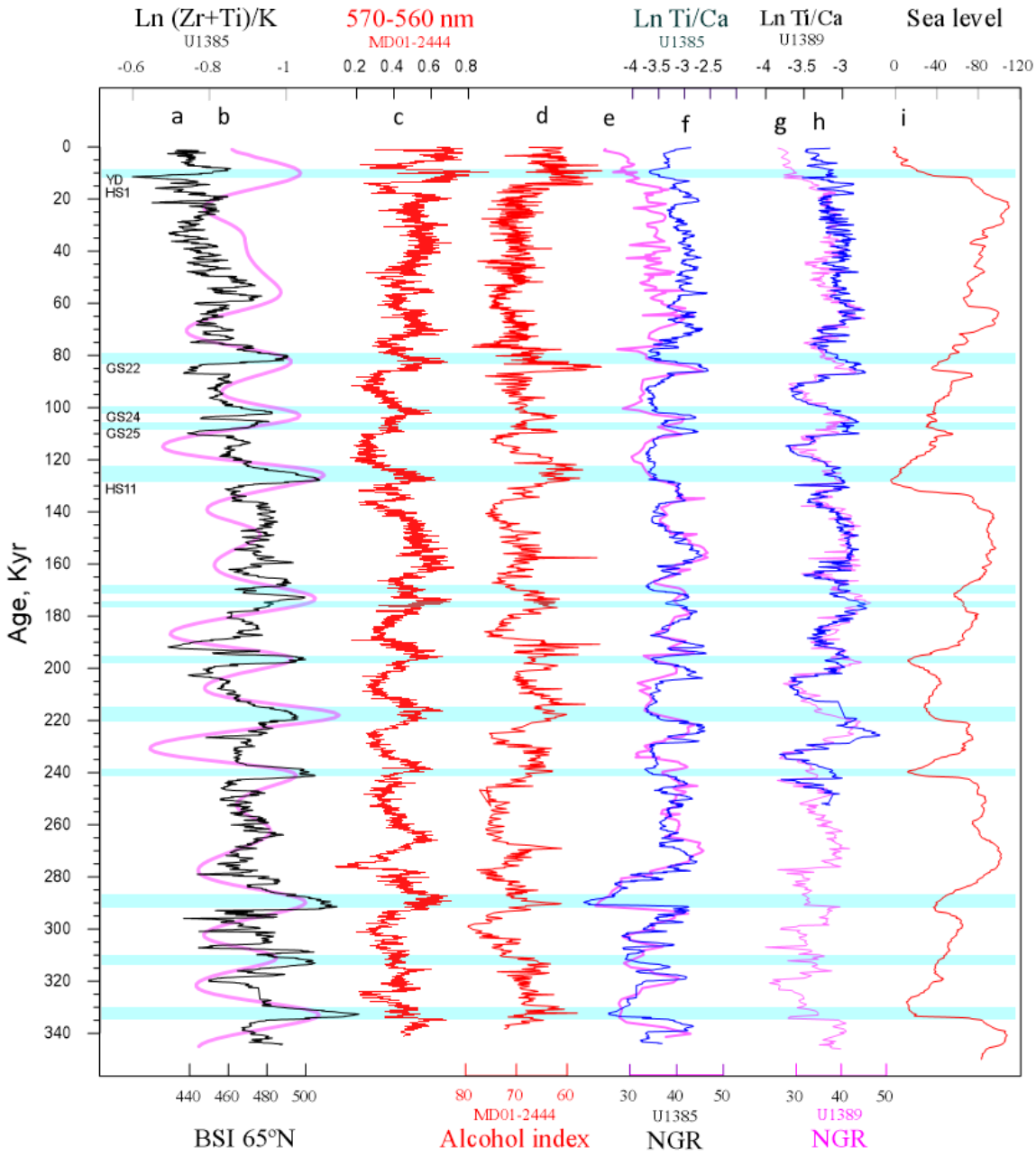

Supplementary Figure 1. Sedimentary property records in several cores of the Iberian Margin

a, Ln (Zr+Ti)/K smooth record at IODP site U1385. **b**, BSI at 65ºN[14]. **c**, First derivative of color reflectance at 570-560 nm in cores MD01-2444/2443, a proxy for sediment redness and hematite content[15]. **d**, Alcohol index record in core MD01-2444/2443 showing the oxidation state of terrestrial organic matter[15]. **e**, Ln Ti/Ca ratio (blue)[13] and **f**, NGR (magenta) smooth records at IODP site U1385[62]. **g**, Ln Ti/Ca ratio (blue) and **h**, NGR (magenta) smooth records at IODP site U1389[62]. **i**, Sea level[63]. Blue bands indicate the winter rainfall events characterized by (Zr+Ti)/K minima (note that scale is inverted). YD = Younger Dryas, HS = Heinrich stadials, GS = Greenland stadial events.

2 Terrestrial input of hematite and oxidized organic particles to the Iberian Margin

To better understand the sources of terrestrial input to the distal setting of the continental rise, where site U1385 was drilled, we focused on two main proxies that vary consistently with the (Zr+Ti)/K ratio at core MD01-2444 and MD01-2443, near IODP site U1385: the hematite proxy (570-560 nm), which reflects the hematite content, and the alcohol index, which reflects the oxidation state of organic matter of terrestrial origin[15] (Supplementary Fig. 1). Both exhibit an almost instantaneous response to precession and were therefore related to low-latitude, wind-driven processes[15]. Two potential sources for higher hematite supply at precession minima were suggested; eolian dust supply from the Sahara or riverine supply from the Tagus or other rivers of southern Portugal and Spain[15]. The alcohol index reflects the relative proportion of n-hexacosanol/(n-nonacosane+n-hexacosanol), two lipid molecules synthesized in cuticle leaf waxes of terrestrial vascular plants that were later transported to the sea[57]. Because n-hexacosanol is more labile, its lower concentration in the sediments and the decrease in the alcohol index are thought to

reflect a higher degradation of organic matter due to greater bottom water ventilation[57] or pore water oxidation.

The relationship between the alcohol index and hematite content[15] (Supplementary Fig. 1) lead us to suggest that the degree of degradation of these organic molecules may reflect more the different supply of labile versus degraded terrestrial organic matter from the continent to the location of core MD01-2444 and MD01-2443 rather than the oxidation processes occurring at the site of deposition. The occurrence of some of the most oxidized levels during the terminal stadial events (Supplementary Fig. 1), which are normally characterized by poor bottom water ventilation, supports this interpretation. Overall, high hematite and low alcohol values in core MD01-2444/2443, near site U1385, occurred during high BSI, but in two distinctive phases (Supplementary Fig. 1). The highest hematite and highest oxidation values are recorded during some of the terminal stadial events, predating BSI maxima (Supplementary Fig. 1). They are followed by a second phase, associated with interstadial events, also characterized by high hematite and low alcohol values that coincide with BSI maxima (Supplementary Fig. 1). While the first phase is characterized by peaks of high (Zr+Ti)/K, the second phase is linked to (Zr+Ti)/K minima. Based on these observations, we assume that the events of hematite-rich sediments and highly oxidized organic particles are related to offshore settling of terrestrial particles from the overlying water column. The first phase was related with open ocean deposition of hematite-rich Saharan dust with degraded, old organic matter as described in the African margin[69]. This could partly explain why the silts contain older organic matter than the clay particles[70]. On the other hand, the strong correlation of low (Zr+Ti)/K with maximum redness and low alcohol index (Supplementary Fig. 1) (during the second phases) can only be explained by a high input of hematite in combination with fine-grained, K-rich clay particles. The presence of clay with high hematite concentrations in a distal environment where carbonate

sedimentation dominates is related here to fluvial flooding events that would generate extensive river plumes reaching the distal setting of Site U1385. These heavy rainfall episodes occurred during warm, interstadial events, synchronous with insolation maxima. This type of sedimentation would be similar to the reddish deposits in the Ceara Rise, which are attributed to increased runoff from the Amazon River during periods of maximum insolation.

The link between climate change on land and terrestrial input to the sea is confirmed by the straight correlation between the events of low siliciclastic input, less redness sediment, more labile organic matter and the expansion of heathland vegetation, which shows the higher percentages at times of low summer insolation. In contrast, the low (Zr+Ti)/K events coincide with the expansion of the Mediterranean forest in the Iberian Peninsula, which typically develops in Mediterranean climates with extreme seasonality[19,20,71,72,73,74,75,76,77]. Summer aridity and heavy winter rainfall promote soil erosion and river flooding, generating extensive river buoyant plumes in the sea.

All these data strongly support that climate variability on the Iberian Peninsula regulated the input of terrestrial particles to the IM and thus the physical properties of the sediments at site U1385, while changes in strength of the MOW played a secondary role. The MOW can cause the resuspension of particles deposited in the slope but cannot change the type of particles reaching the IM from the continent. Bottom currents can mobilize sortable silt particles along the continental slope but cannot discriminate between hematite-rich or hematite-poor silts.

Paleoflood records in fluvial sediments from the Tagus and Duero rivers, the main rivers of the Iberian Peninsula draining to the Atlantic, also revealed the occurrence of numerous extreme flood episodes during the early Holocene while these events were rare during the YD and the middle to late Holocene[78].

References

59. Oliveira, A., Santos, A. I., Santos, R. & Zacarias, N. Nepheloid layer dynamics overview of the Portuguese continental shelf. *Cont. Shelf Res.* **261**, 105027 (2023).

60. Lofi, J. *et al.* Quaternary chronostratigraphic framework and sedimentary processes for the Gulf of Cadiz and Portuguese Contourite Depositional Systems derived from Natural Gamma Ray records. *Mar. Geol.* **377**, 40–57 (2016).

61. Thomson, J. *et al.* Implications for sedimentation changes on the Iberian margin over the last two glacial/interglacial transitions from (Th-230(excess))(0) systematics. *Earth Planet. Sci. Lett.* **165**, 255–270 (1999).

62. Expedition 339 Scientists. Site U1385. in *Proceedings of the Integrated Ocean Drilling Program* (ed. Stow Hernández-Molina, F.J., Alvarez Zarikian, C.A., and the Expedition 339 Scientists, D. A. V) vol. 339 (Integrated Ocean Drilling Program Management International, Inc., 2013).

63. Grant, K. M. *et al.* Sea-level variability over five glacial cycles. *Nat. Commun.* **5**, (2014).

64. Lourens, L. J., Wehausen, R. & Brumsack, H. J. Geological constraints on tidal dissipation and dynamical ellipticity of the Earth over the past three million years. *Nature* **409**, 1029–1033 (2001).

65. Konijnendijk, T. Y. M., Ziegler, M. & Lourens, L. J. Chronological constraints on Pleistocene sapropel depositions from high-resolution geochemical records of ODP Sites 967 and 968. *Newsletters Stratigr.* **47**, 263–282 (2014).

66. Moreno, T. *et al.* Geochemical variations in aeolian mineral particles from the Sahara–Sahel Dust Corridor. *Chemosphere* **65**, 261–270 (2006).

67. Klaver, M. *et al.* Reliability of detrital marine sediments as proxy for continental crust composition: The effects of hydrodynamic sorting on Ti and Zr isotope systematics. *Geochim. Cosmochim. Acta* **310**, 221–239 (2021).

68. Nichols, M. D. *et al.* Climate-Induced Variability in Mediterranean Outflow to the North Atlantic Ocean During the Late Pleistocene. *Paleoceanogr. Paleoclimatology* **35**, e2020PA003947 (2020).

69. Eglinton, T. I. *et al.* Composition, age, and provenance of organic matter in NW African dust over the Atlantic Ocean. *Geochemistry, Geophys. Geosystems* **3**, 1–27 (2002).

70. Magill, C. R. *et al.* Transient hydrodynamic effects influence organic carbon signatures in marine sediments. *Nat. Commun.* **9**, 8 (2018).

71. Margari, V. *et al.* Land-ocean changes on orbital and millennial time scales and the penultimate glaciation. *Geology* **42**, 183–186 (2014).

72. Cutmore, A. *et al.* Abrupt intrinsic and extrinsic responses of southwestern Iberian vegetation to millennial-scale variability over the past 28 ka. *J. Quat. Sci.* **37**, 420–440 (2022).

73. Sánchez Goñi, M. F., Eynaud, F., Turon, J. L. & Shackleton, N. J. High resolution palynological record off the Iberian margin: direct land-sea correlation for the Last Interglacial complex. *Earth Planet. Sci. Lett.* **171**, 123–137 (1999).

74. Oliveira, D. *et al.* Unraveling the forcings controlling the vegetation and climate of the best orbital analogues for the present interglacial in SW Europe. *Clim. Dyn.* **51**, 667–686 (2018).

75. Oliveira, D. *et al.* Combination of insolation and ice-sheet forcing drive enhanced humidity in northern subtropical regions during MIS 13. *Quat. Sci. Rev.* **247**, 106573 (2020).

76. Sánchez Goñi, M. F. *et al.* Tropically-driven climate shifts in southwestern Europe during MIS 19, a low eccentricity interglacial. *Earth Planet. Sci. Lett.* **448**, 81–93 (2016).

77. Gomes, S. D. *et al.* Time-transgressive Holocene maximum of temperate and Mediterranean forest development across the Iberian Peninsula reflects orbital forcing. *Palaeogeogr. Palaeoclimatol. Palaeoecol.* **550**, (2020).

78. Benito, G. *et al.* Late Pleistocene–Holocene multi-decadal patterns of extreme floods in NW Iberia: The Duero River palaeoflood record. *Quat. Sci. Rev.* **321**, 108356 (2023).

Extended data Figure 5. Surface water freshening in the westernmost Mediterranean during deposition of S9.

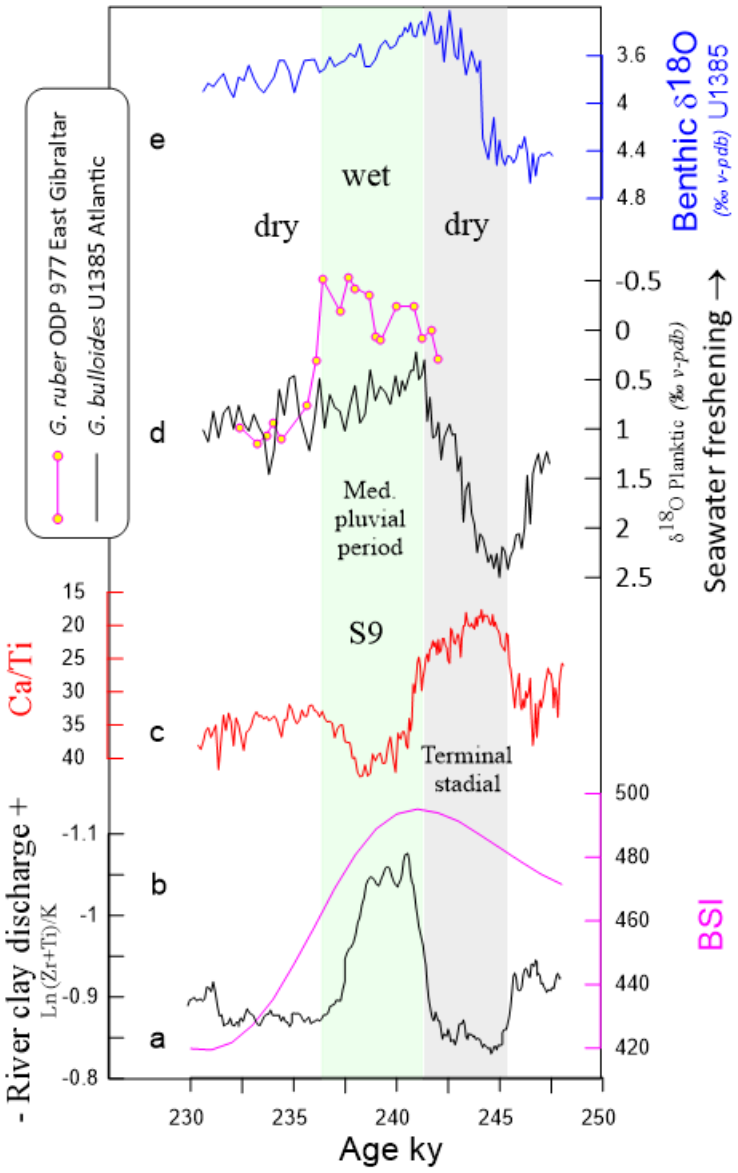

Extended data Figure 5

a, BSI at 65ºN[14]. **b**, Ln (Zr+Ti)/K record of river clay discharge at site U1385. **c**, Ca/Ti record from site U1385. **d**, Sea surface water freshening events shown by *G. ruber* $\delta^{18}O$ drops. *G. ruber* $\delta^{18}O$ record from ODP 977 in the westernmost Mediterranean (magenta)[40]; *G. bulloides* $\delta^{18}O$ from site U1385 (black) (eastern Atlantic)[41]; **e**, Benthic $\delta^{18}O$ record from site U1385 (eastern Atlantic)[41]. The gray and green bands show the Terminal stadial event and the Mediterranean pluvial period, respectively.